Photofragment Translational Spectroscopy of CH_2I_2 at 304 nm: Polarization Dependence and Energy Partitioning

Kwang-Woo Jung*, Temer S. Ahmadi†, and Mostafa A. El-Sayed‡

**Department of Chemistry, Wonkwang University, Iksan 570-749, Korea*
†Work done in partial fulfillment of the Ph.D. requirements from the University of California, Los Angeles
‡School of Chemistry and Biochemistry, Georgia Institute of Technology, Atlanta, Georgia 30332-0400, U. S. A.
Received July 24, 1997

The photodissociation dynamics of CH_2I_2 has been studied at 304 nm by state-selective photofragment translational spectroscopy. Velocity distributions, anisotropy parameters, and relative quantum yields are obtained for the ground $I(^2P_{3/2})$ and spin-orbit excited state $I^*(^2P_{1/2})$ iodine atoms, which are produced from photodissociation of CH_2I_2 at this wavelength. These processes are found to occur *via* $B_1 \leftarrow A_1$ type electronic transitions. The quantum yield of $I^*(^2P_{1/2})$ is determined to be 0.25, indicating that the formation of ground state iodine is clearly the favored dissociation channel in the 304 nm wavelength region. From the angular distribution of dissociation products, the anisotropy parameters are determined to be $\beta(I)=0.4$ for the $I(^2P_{3/2})$ and $\beta(I^*)=0.55$ for the $I^*(^2P_{1/2})$ which substantially differ from the limiting value of 1.13. The positive values of anisotropy parameter, however, show that the primary processes for I and I* formation channels proceed dominantly *via* a transition which is parallel to I-I axis. The above results are interpreted in terms of dual path formation of iodine atoms from two different excited states, *i.e.*, a direct and an indirect dissociation via curve crossing between these states. The translational energy distributions of recoil fragments reveal that a large fraction of the available energy goes into the internal excitation of the CH_2I photofragment; $\langle E_{int}\rangle/E_{avl}=0.80$ and 0.82 for the I and I* formation channels, respectively. The quantitative analysis for the energy partitioning of available energy into the photofragments is used to compare the experimental results with the prediction of direct impulsive model for photodissociation dynamics.

Introduction

Investigations on the photodissociation dynamics of alkyl iodides in the low-lying absorption band have yielded detailed information about the energy partitioning in photofragments, branching ratios for $I^*(^2P_{1/2})$ to $I(^2P_{3/2})$ formation, and the product angular distributions with respect to the electric field vector.[1-6] Alkyl iodides have received substantial attention for systematic study of photodissociation since very rapid dissociations along the repulsive states[7,8] offer a chance to monitor the effects of molecular and electronic structures on dynamics. The ultraviolet absorption spectra of monoiodoalkanes generally contain a broad and structureless band around 260 nm, corresponding to excitations to three electronic states $^3Q_1$, $^3Q_0$, and $^1Q_1$, of which the $^3Q_0 \leftarrow X$ transition usually dominates.[1,9] All these transitions are attributed to excitation of an electron from a lone pair nonbonding orbital in the iodine atom to the σ^* antibonding orbital localized in the C-I bond. The repulsive nature of the excited states produces either a ground-state I ($^2P_{3/2}$) atom (denoted as I) or a spin-orbit excited-state $I(^2P_{1/2})$ atom (denoted as I*) and radical fragments with varying degrees of internal (usually rovibrational) excitation.

The electronic states involved and ultraviolet photodissociation dynamics of diiodoalkanes have long been the object of interest and controversy.[2,10-16] The absorption spectrum of CH_2I_2 consists of three relatively broad features that have been decomposed into four or five bands with peaks around 214, 249, 285, and 311 nm.[10,11] A simple exciton model given by Kawasaki *et al.*[2] shows that there are at least five electronic states involved in the ultraviolet absorption spectrum. Subsequent magnetic circular dichroism (MCD) spectrum obtained by Gedanken and Rowe[11] suggested the presence of five distinct bands and a weak shoulder at 312 nm, which was attributed to a forbidden transition. The energetically possible dissociation processes in the ultraviolet are

$$CH_2I_2 + h\nu_{uv} \rightarrow \begin{cases} CH_2I + I(^2P_{3/2}), & (1) \\ CH_2I + I^*(^2P_{1/2}), & (2) \\ CH_2(\tilde{a}^1A_1) + I_2(X^1\Sigma_g^+). & (3) \end{cases}$$

The dominant photodissociation process for diiodomethane with ultraviolet excitation is the bond rupture of one of the C-I bonds to give a CH_2I radical and either a ground-state I or an electronically excited I* atom. Although process (3) is energetically possible at wavelength shorter than 333 nm, this process is forbidden by symmetry.[14,17] This has been confirmed experimentally by Schmitt and Comes,[18] although electronically excited I_2 does occur in the vacuum ultraviolet.[16]

Kawasaki *et al.*[2] used molecular beam photofragmentation to show that excitation of the low-lying electronic states of CH_2I_2 (both with B_1 symmetry) directly dissociates to give I or I* atom and the rovibrationally excited CH_2I radical in a shorter time as compared to the period of molecular rotation. Translational photofragment spectroscopy experiments by Kroger *et al.*[15] indicated that CH_2I radical is formed with a large degree of internal excitation in the photodissociation of 265-340 nm region. Leone *et al.*[19,20] extended this work

*Author to whom correspondence should be addressed.

and measured the vibrational energy distributions of CH_2I photodissociation product by time- and wavelength- resolved infrared emission spectroscopy and obtained wavelength-specific I* quantum yields for CH_2I_2 in the region of 248-340 nm. In that work the I* yields could not be reconciled with a simple deconvolution of the absorption spectrum into component gaussian bands. They suggested that processes (1) and (2) dominate, which is in agreement with the symmetry restriction but a curve-crossing mechanism is operative in the photodissociation pathways.

Photofragment translational spectroscopy of dissociating molecules such as alkyl[21~23] and arlyl[24~28] halides has been proven to be a very useful tool in characterizing both the ground and excited state potential energy surfaces. Especially when coupled with a study of the anisotropy parameters of the dissociating channels, great insight can be gained about the photodissociation dynamics involved.

In this paper we investigate the photodissociation of CH_2I_2 at 304 nm in order to determine the angular and translational energy release. distributions of photofragments. The quantum yields for I and I* formation channels are also determined by state-selective photofragment translational spectroscopy. Such results, along with the measurements of the anisotropy parameter provide more complete understanding on the correlation between the electronic states and photofragment pathways in this molecule at this wavelength.

Experimental

The experimental set up, similar in design to that described previously,[29] consists of a supersonic beam source and a home built time-of-flight mass spectrometer (TOFMS). The gas mixture for the molecular beam is prepared by passing He over liquid CH_2I_2 sample (*ca.* 1 Torr vapor pressure at room temperature) to make a total pressure of 400 Torr. Gaseous CH_2I_2 molecules are introduced through a 0.5 mm diameter pulsed valve (General Valve) into the source chamber, which is pumped by a 4 in. diffusion pump. The source chamber is separated from the main chamber by a 1.0 mm diameter skimmer located 20 mm from the nozzle. The molecular beam has a 10 Hz repetition rate and 400 Torr stagnation pressure. The pressure in the source and main chamber are always below 1.0×10^{-6} and 5.0×10^{-7} Torr, respectively.

CH_2I_2 molecules from a pulsed molecular beam are photodissociated by a linearly polarized nanosecond laser pulse to produce iodine atom and CH_2I radical. Photodissociation experiments are performed at polarization parallel and perpendicular to the detection axis, *i.e.*, polarization angles of $\alpha=0°$ and $\alpha=90°$, respectively. For the 304 nm dissociation experiments, the iodine atoms are produced in either the ground or spin-orbit excited states and are state selectively ionized within the same laser pulse (304.67 nm for I and 304.02 nm for I* detection). The iodine ions are then allowed to move in a field free region for a delay time of about 2 μs. During the delay time the photoions spread out from their initial positions (*i.e.* laser focus) according to their recoil velocities and produce a spatial distribution. After a delay from each laser pulse, the photoions are accelerated toward the detector by a pulsed acceleration voltage of approximately 1400 V applied for 1 μs to a repelling electrode in the TOFMS. The ion packet travels across a field free region to a discrimination pinhole 4.0 mm in diameter placed in front of the detector to reduce the detection solid angle. The arrival time of an ion to the detector is then a function of its initial position prior to the application of the acceleration field. Consequently, the arrival time distribution of the ion packet at the detector is directly related to the recoil velocity distribution of neutral fragment along the detection axis.

Methylene iodide was obtained from Aldrich and used without further purification. Prior to use the sample underwent several freeze-pump-thaw cycles, thus, removing lower vapor pressure contaminant molecules. The space-charge effect between ionized photofragments is minimized by adjusting the laser power to a maximum of 0.1 mJ/pulse. To ensure that there was no significant multiphoton processes occurring, experiments were performed with similar laser power at wavelengths slightly off resonance from the I and I* resonance absorption wavelengths of 304.67 and 304.02 nm. No multiphoton ionzation was observed. It is also necessary to eliminate the interference from clusters since the photofragments from clusters exhibit broader velocity distributions than monomer molecules do.[5,30] Therefore, we have minimized the contribution from clusters by choosing only the early part of the molecular beam pulse for photolysis.

Results

Figure 1 presents the laboratory velocity distributions in the z (detection axis) direction for the $I(^2P_{3/2})$ and $I^*(^2P_{1/2})$ photofragments produced upon the photodissociation of CH_2I_2 at (a) 304.67 and (b) 304.02 nm, respectively. The peaks at positive and negative velocities correspond to iodine atoms whose initial recoil velocities are toward and away from the detector, respectively. In each figure, the upper and lower traces correspond to photolysis laser polarizations parallel ($\alpha=0°$) and perpendicular ($\alpha=90°$) to the detection axis. The photon energy at 304 nm corresponds to 94 kcal/mol. Thus, on thermodynamic grounds, the primary dissociation caused by photons in the 304 nm photolysis of CH_2I_2 could produce either I/I* atoms or I_2 molecules. The energetics of the possible photodissociation pathways of CH_2I_2 and its photofragments, estimated from the thermochemical data,[19] are listed in Table 1. In the present study, however, there is no evidence for the molecular elimination channel to form I_2 since no ion signal from I_2 was observed where it would appear at $\upsilon=1100$ m/sec.

At least two types of velocity distributions are clearly observed for I formation channel, indicating that the I formation channel consists of two different dissociation processes. The ion signal of high-velocity component (υ_z~ 550 m/s) at $\alpha=0°$ is *ca.* twice as strong as that at $\alpha=90°$. The result suggests that the major I fragments having a high-velocity component recoil preferentially parallel to the direction of the electric vector of the excitation transition. It should be noted that the high-velocity peak stems from the iodine atoms resulting from the primary dissociation process (1).

The similar intensity of the low-velocity peak at the two laser polarization angles is suggestive of an isotropic

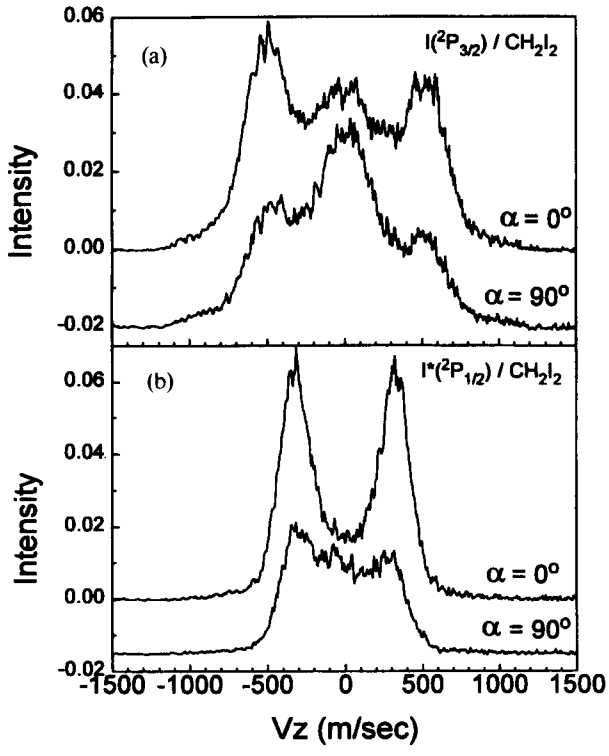

Figure 1. The lab. velocity (υ_z) distributions of resonantly-ionized (a) ground-state and (b) spin-orbit excited-state iodine photofragments produced from photodissociation of CH_2I_2 at 304.67 and 304.02 nm, respectively. The negative and positive velocity peaks correspond to the iodine atoms whose initial recoil velocity is either away from or toward the detector. The notation $\alpha=0^0$ and $\alpha=90^0$ refers to parallel and perpendicular polarization of the electric vector of the dissociating laser with respect to the detection axis. For I dissociation channel, the outside peaks exhibit high recoil velocities and anisotropic character. The broader inner velocity distributions have very low recoil velocities and isotropic behavior.

character of I atoms formed from this channel. The low-velocity peak of the I atoms could result from several dissociation routes as discussed below. The spontaneous secondary decay of the hot CH_2I radicals which possess sufficient internal energy may produce slow-velocity distribution of I atoms. As summarized in Table 1, the dissociation energy for the channel which leads to $CH_2I \rightarrow CH_2+I$ is rather large (D_0^0=61.4 kcal/mol). After primary C-I bond breakage requiring 50.1 kcal/mol, the CH_2I product cannot be left with enough internal energy to undergo unimolecular dissociation to form CH_2+I. As a consequence, the three-body dissociation process either from the sequential or consecutive decay has a higher threshold in CH_2I_2 and is not accessible at the present photolysis wavelength.

As another possible route to produce low velocity I atoms, CH_2I fragments formed from the primary process can undergo secondary photodissociation as a result of absorbing another photon:

$$CH_2I^* + h\nu \rightarrow CH_2 + I \qquad (4)$$

During the nanosecond duration of the laser pulse, there is ample time for vibronically hot CH_2I radicals to absorb a second photon, dissociating to CH_2+I fragments. The low recoil velocity of the I atom could be a result of the nature of the excited state of the CH_2I radical that might lead to a slower dissociation or due to the conservation of linear momentum of CH_2 and I photofragments. In addition, more effective collection efficiency of slow-velocity component than fast-velocity component in our detection scheme produces the intense peak in the slow velocity region. The observed isotropic character of this formation channel can thus result from either the slow dissociation or the loss of angular dependence after the primary dissociation process.

Table 1. Energetics of Possible Photodissociation Pathways of CH_2I_2 and its Photofragments[a]

Dissociation channels	Dissociation Energy[b], D_0^0	E_{avl}[c]
$CH_2I_2 \rightarrow CH_2I+I(^2P_{3/2})$	50.1	43.7
$\rightarrow CH_2I+I^*(^2P_{1/2})$	71.8	22.2
$\rightarrow CH_2(\tilde{a}^1A_1)+I_2(X\Sigma_g^+)$	84.6	~9.4
$CH_2I \rightarrow CH_2(X^3B_1)+I(^2P_{3/2})$	61.4	
$\rightarrow CH_2(X^3B_1)+I^*(^2P_{1/2})$	83.1	
$CH_2I_2 \rightarrow CH_2(X^3B_1)+I(^2P_{3/2})+I(^2P_{3/2})$	112.7	
$\rightarrow CH_2(X^3B_1)+I(^2P_{3/2})+I^*(^2P_{1/2})$	134.2	

[a] Energies are in kilocalories per mol. [b] D_0^0 is obtained by subtracting the thermal energy from the bond dissociation energy at 298 K.[33] [c] E_{avl} is the amount of excess energy available for translational and internal excitation after a single-photon dissociation at 304.67 nm (for I) and 304.02 nm (for I*).

A second possible route that could produce the slow $I(^2P_{3/2})$ could involve the multiphoton absorption by the parent molecule itself to lead to statistical dissociation of the parent ion.

$$CH_2I_2 + nh\nu \rightarrow CH_2I_2^+ \rightarrow CH_2I + I^+ \qquad (5)$$

The statistical dissociation would give rise to iodine ions of low translation energy and with near zero β value. Thus the mechanism can be tested since changing the laser wavelength slightly to become off resonance from the (2+1) photon ionization of iodine atoms should not affect the intensity of the low velocity iodine signal. Carrying out this experiment is found to eliminate the iodine recoil velocity spectrum. This eliminates the multiphoton absorption of the parent molecules as the source of iodine atom signal observed.

Figure 1b gives the velocity distributions of iodine ion measured at 304.02 nm with polarization angles $\alpha=0^o$ and $\alpha=90^o$. At this wavelength, the excited-state iodine atom I* can only be selectively ionized. Contrasting to the I formation channel, the I* velocity distribution shows only one peak at υ_z~350 m/s, indicating that secondary photodissociation reaction plays a minor contribution to the I* formation presumably due to the small amount of excess energy of CH_2I radical and also its dissociation pathway. The intensity difference of I* signals is even greater at the two laser polarization angles as compared with the case of I photofragment. This result indicates that the angular distribution of the I* atom has also an anisotropic character of dominant transition dipole vector μ oriented parallel to the line connecting the two iodine atoms of CH_2I_2.

The angular distribution as well as the energy partitioning between internal excitation and relative translation of the photoproducts affects the velocity component distribution and its peak shape. From the measured lab. recoil velocity distributions, $F(\upsilon, \theta)$, at two different polarization angles, the recoil anisotropy parameters $\beta(\upsilon)$ and the recoil speed distributions $G(\upsilon)$ can be determined according to the following equation:[23]

$$F(\upsilon, \theta)=\frac{1}{4\pi}[1+\beta(\upsilon)P_2(\cos\theta)]G(\upsilon) \quad (6)$$

where $P_2(\cos\theta)=(3\cos^2\theta-1)/2$ is the second-order Legendre polynomial and θ is the lab. recoil angle with respect to the electric vector of the polarized light. For prompt dissociation of unmixed absorption, the β value is -1 or $+2$ if the molecular transition dipole moment axis of the absorbing transition is lying either perpendicular or parallel to the dissociation bond axis. The β value lies in between -1 and $+2$ for absorption of mixed polarization. The $G(\upsilon)$ and $\beta(\upsilon)$ for I and I* atoms are calculated using a deconvolution technique[31] and presented in Figure 2. The $G(\upsilon)$ distributions of I and I* atoms show quite interesting features. The recoil speed distribution of I and I* atoms are broad as compared to the monoiodoalkanes[5,6,25,26] studied to date and their maxima are not located at high recoil speeds. In addition, the recoil speed of I photofragments appears up to the maximum value (υ_{max}=1200 m/sec) which is available after a 304 nm photoexcitation. This is suggestive of the fact that a small fraction of the excited CH_2I_2 molecules behaves as the corresponding monochromophoric molecule, in this case CH_3I,

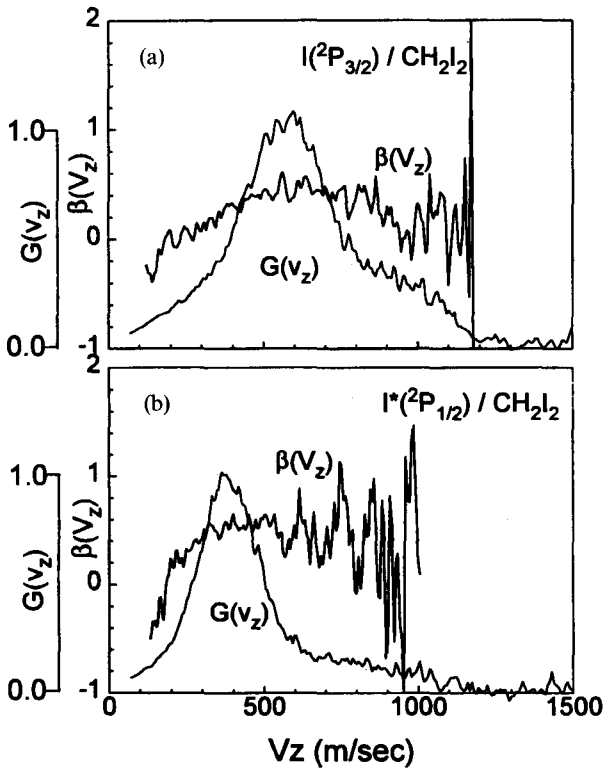

Figure 2. The lab. recoil velocity distributions $G(\upsilon)$ and the anisotropy parameters $\beta(\upsilon)$ of I and I* photodissociation channels obtained from the recoil velocity distributions in Figure 1.

where about 90% of the available energy is released into the translational energy of photofragments.[32-34]

The measured ion signal ratio of I* to I is proportional to the branching ratio between I* and I atoms by

$$N(I^*)/N(I)=k\,S(I^*)/S(I) \quad (7)$$

where S refers to the integrated intensity, obtained from the appropriate $G(\upsilon)$ distribution, N is the number of iodine atoms resulting from photodissociation, and k is the proportionality constant. The relative sensitivity (k=0.769) value for detecting I and I* atoms was obtained from the system calibration using I_2 as a standard molecule.[35] The branching ratio, $N(I^*)/N(I)$, of CH_2I_2 at 304 nm is found to be 0.33. Using the relation between the branching ratio and the relative quantum yields Φ^* ($=N(I^*)/[N(I^*)+N(I)]$), we obtain Φ^*=0.25 for the excited-state iodine atom, which is in good agreement with the result of Baughcum and Leone[19] on CH_2I_2 photodissociation at 308 nm ($\Phi^*=0.25\pm0.02$). The result implies that the production of ground state iodine is clearly the favored channel in the 304 nm wavelength region.

The anisotropy parameters $\beta(\upsilon)$ of I and I* atoms in Figure 2 provide further details for the nature of electronic transitions of CH_2I_2 molecule. The angular distributions of the I and I* fragments exhibit a parallel character in both channels. The observed anisotropic parameter of I formation channel is $\beta(I)$=0.4. This is slightly less anisotropic than I* formation, $\beta(I^*)$=0.55. The positive β values can then be attributed to the dominant contribution from the transition which is parallel to I···I axis. The $\beta(I)$ for the low velocity distribution is near zero value.

The distributions of the total translational energy release, $G(E_t)$, of the I and I* dissociation channels are obtained from $F(\upsilon, \theta)$ by the use of equation (8) which is derived by applying the conservation of linear momentum during the photodissociation process at two recoil angles. These are displayed in Figure 3.

$$G^{\theta}(E_t)=\frac{m_R}{m_1(m_1+m_R)}\frac{F(\upsilon, \theta),}{\upsilon} \quad (8)$$

where E_t is the total translational energy of the iodine atom and the CH_2I radical and m_1 and m_R are the masses of the iodine atom and that of the CH_2I radical, respectively. The available energies, E_{avl} and E^*_{avl} for I and I* formation channels can be determined from the energy conservation relations:

$$E_{avl}=h\nu-D_0^0+E^p_{int}=E_t+E_{int} \quad \text{for the I formation} \quad (9)$$

$$E^*_{avl}=E_{avl}-E_{so}=E^*_t+E^*_{int} \quad \text{for the I* formation} \quad (10)$$

where $h\nu$ is the photon energy, D_0^0 the dissociation energy of CH_2I_2 into the CH_2I radical and the I atom at 0 K (50.1 kcal/mol), E^p_{int} the internal energy of the parent molecule, and E_{so} the spin-orbit excitation energy of iodine atom (21.7 kcal/mol). D_0^0 is obtained by subtracting the thermal energy [36] from the bond dissociation energy at 298 K.[2] After dissociation, the available energy partitions into the internal energy (E_{int}) of the CH_2I radical and the total center-of-mass translational energy of the photofragments (E_t). E^p_{int} of the parent molecules in the supersonic molecular beam can be neglected for the calculation. The E_{avl} and E^*_{avl} for two dis-

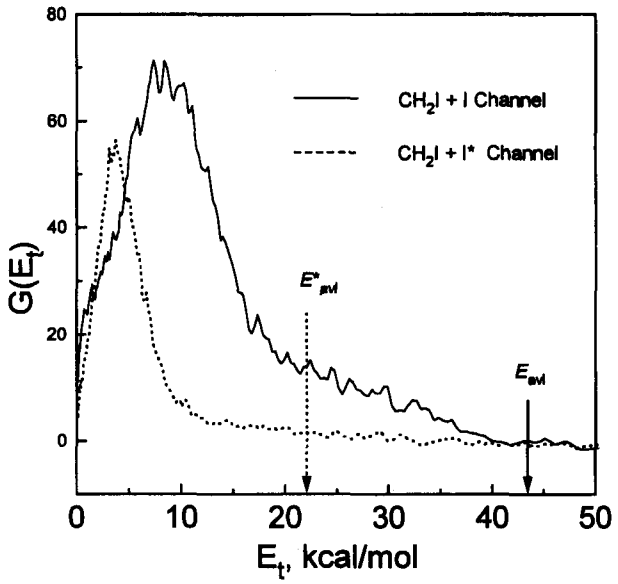

Figure 3. Translational energy release distributions $G(E_t)$ of the I and I* photodissociation channels. The $G(E_t)$ distributions are obtained from the lab. velocity distributions in Figure 2 by using an instrumental detection function described in Ref. 31. The distributions show the average translational energies of 3.9 (for the I* channel) and 8.7 kcal/mol (for the I channel).

sociation channels are indicated by vertical arrows in Figure 3. The observed most probable translational energies $<E_t>$ are summarized in Table 2 together with the available energy and the energy partitioning. As shown, the total translational energy of the photofragments is rather small compared to the available energy of each dissociation channel. From the fact that the energy separation (4.8 kcal/mol) of these two peaks is smaller than the iodine spin-orbit splitting of 21.7 kcal/mol we infer that the CH_2I fragments formed from the I formation channel contain more internal energy than the CH_2I formed from the energetically less favorable I* channel.

Discussion

Molecular orbital considerations for CH_2I_2 using a simple exciton model predict the lowest excited electronic states to be $B_1\sigma$, $B_1\pi$, $B_2\pi'$, $A_1\pi$, and $A_1\sigma$ symmetry, in order of increasing energy.[2] Kawasaki *et al.*[2] calculated the β value for transitions polarized along the three axis in CH_2I_2. Only the transition polarized along the I···I axis is found to have a positive β value near unity. Magnetic circular dichroism spectra obtained by Gendanken and Rowe[11] suggest the presence of five distinct bands and a weaker shoulder, which is attributed to a forbidden transition. Koffend and Leone[14] have measured the relative yield of spin-orbit excited iodine atoms from the photodissociation of CH_2I_2 as a function of the photolysis wavelength. They concluded that the lowest electronic transition (~310 nm) yields ground-state I atoms, whereas the next higher subband in the 285 nm range yields both ground and spin-orbit excited I atoms, most probably due to a curve-crossing mechanism.

Table 2. Partitioning of the Available Energy in the photodissociation of CH_2I_2[a]

Iodine state	λ_{ex} (nm)	E_{avl}	$<E_t>$	$<E_{int}>/E_{avl}$		
				exp[b]	soft[c]	rigid[d]
I	304.67	43.7	8.7	0.80	0.84	0.77
I*	304.02	22.2	3.9	0.82	0.84	0.77

[a] Energies are in kilocalories per mole. [b] $<E_{int}>/E_{avl}$ measured in this work. [c] $<E_{int}>/E_{avl}$ impulsive model calculated on the basis of the soft radical limit. [d] $<E_{int}>/E_{avl}$ impulsive model calculated on the basis of the rigid radical limit.

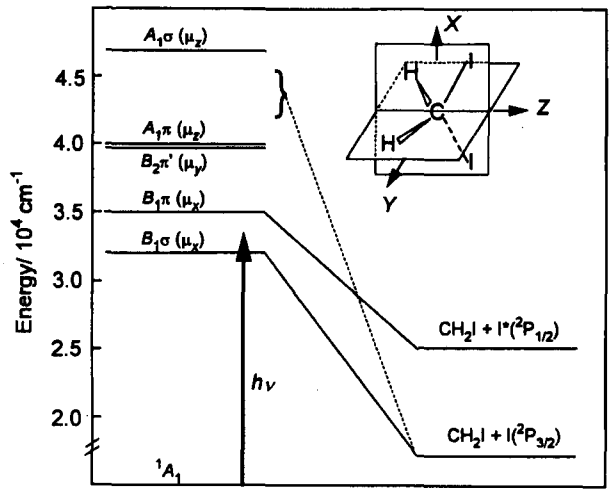

Figure 4. Energy correlation diagram for the low-lying excited states of CH_2I_2 based on the results from Refs. 2, 4, and 14. The insert shows a geometry of CH_2I_2 indicating the orientation of the transition dipole moment (μ). The vertical arrow indicates photoexcitation of 304 nm wavelength.

Figure 4 shows the energy correlation diagram for several low-lying electronic states of CH_2I_2 based on the results from Refs. 2, 4, and 14. The model of Kawasaki *et al.*[2] suggests that the two lowest states of CH_2I_2 have B_1 symmetry. The first $B_1\sigma$ state is excited with the transition moment μ_x parallel to line connecting the two I atoms. They suggested that such a transition should produce mainly ground-state I ($^2P_{3/2}$) atoms. This prediction is also confirmed by Koffend and Leone[14] that no I* production is observed below 340 nm. Excitation at 304 nm would be close to the peak of the first absorption band, but the second excited $B_1\pi$ state would begin to play an important role due to overlapping absorption between the two states.[19] Our results clearly indicate that CH_2I_2 molecule undergoes a two-body dissociation yielding CH_2I radical and I or I* atom. This provides evidence for the presence of two electronic excited states (both with B_1 symmetry) that are correlated with the photodissociation channels of CH_2I+I and CH_2I+I*. Although the energetics would allow for the creation of I_2 in the electronic ground state the fact that we did not observe iodine atoms of recoil component faster than that observed from I_2 photolysis[37] (1100 m/s) eliminates this channel for the iodine atom production in the present study. Furthermore, providing retention of C_{2v} symmetry during dissociation, symmetry considerations reveal that the B_1 excited state does not correlate with stable and energetically accessible states of I_2. For CH_2I_2 the I_2 molecular channel is,

therefore, unlikely to be active.

The magnitude and sign of β provide information with regard to the orientation of the transition dipole moment μ in the parent molecule, the symmetry of the excited state and the excited state lifetime. The C_{2v} symmetry of CH_2I_2 permits three possible orientations of the transition dipole moment, corresponding to the *y* (perpendicular to the ICI plane), *z* (bisecting the ICI angle), and *x* (parallel to the I-I direction) axis directions. The insert in Figure 4 shows the geometry of CH_2I_2 molecule. The anisotropy parameters for these three orientations can be calculated in the limiting case of instantaneous recoil by applying the following relation,

$$\beta = 2P_2(\cos\Theta), \tag{11}$$

where Θ is the angle between the dissociation bond axis and the transition dipole moment μ. The positive values for the observed anisotropy parameter β of I and I* fragments imply that the transition dipole vector μ is oriented parallel to recoil direction.

The observed anisotropy parameters substantially differ from the limiting value, *i.e.*, +1.13 for the parallel transition, taking into account the C_{2V} symmetry of the parent molecule.[2] Emission spectroscopy of CH_2I_2 done by Zhong and Imre[38] indicated that, on the first excited state, CH_2I_2 dissociates directly on a time scale slightly longer than that for CH_3I. From the observation of the I-C-I bending fundamental, they also reported that the bond angle changes early in the dynamics. In a very recent study on the resonance Raman spectra of CH_2I_2, Kwok and Phillips[39] also found that the breaking of the C-I bond is substantially slower than in any alkyl iodide previously studied. In light of these observations, one concludes that the decrease in the anisotropy parameter observed for the iodine produced in this channel from its limiting value of +1.13 is a result of depolarization resulting from the rotation and distortion of the excited molecule prior to dissociation. Alternatively, the formations of I and I* atoms could result from absorption to more than one state with different orientation of the transition dipole moment. This could lead to the observed low value of anisotropy parameters. This would require a large decrease in the energy of the higher A_1 or B_2 states calculated by the exciton model.[2]

Quantum yield for I* production provides direct information on the dissociative channels in the photofragmentation process. Hunter *et al.*[12] measured the quantum yield of I* from CH_2I_2 photodissociation by employing an optoacoustical technique in the wavelength region of 247.5-365.5 nm. They found that the first band (λ=~310 nm) correlated with production of only $I(^2P_{3/2})$; the second band (λ=~288 nm) had contributions from both I* and I with a I/I* ratio of 1.75; while the third band (λ=~249 nm) had contributions almost equally from I* and I, I/I*=1.1. They assigned B_1 symmetry to the two low energy bands and A_1 to the third band. However, results of I* quantum-yield at 308-348 nm could not be explained simply on the basis of a Gaussian deconvolution. For example, with the simple Gaussian fit, 92% of the absorption peak at 248 nm should be to a single state, yet the observed Φ_{I^*} is only 0.46. At 308 nm, the I* yield is only ~1/3 of the best-fit Gaussian amplitude[14,40] the basis of the rigid radical limit.

comes important for the second and other high excited states.

As described earlier, the only two lowest electronic states (B_1 symmetry) can be accessed by the excitation of 304 nm. Therefore, our observation of Φ^*=0.25 is explained by proposing that I atoms originate from a mixed transition ($B_1\sigma$ and $B_1\pi$ states *via* polarization which is parallel to I···I axis) whereas I* atoms are produced from the $B_1\pi$ excited state. Since the $B_1\pi$ state correlates with the I* formation channel (see Figure 4), the curve crossings between $B_1\pi$ and higher excited state must occur to produce I atoms in the photodissociative channels.[14,19] The results are summarized in Table 3. Unfortunately, no calculated excited state surface of CH_2I_2 are available to date.

The translational energy release distribution has much smaller width (fwhm ≈ 4.5 kcal/mol) in the I* formation channel than that for the I channel (fwhm ≈ 11.2 kcal/mol), as shown in Figure 3. This suggests that the internal energy left in the CH_2I radical is distributed more narrowly for the I* channel than the I channel. This behavior can be explained by the difference in the internal energy available in two channels. Since the I* channel carries an extra 21.7 kcal/mol compared to the I channel, the total available energy for the radical fragment becomes much smaller in this case. The larger the available energy, the more ways the energy can be distributed and the broader would be the internal energy distribution in CH_2I radical.

The translational energy release has been measured to be very high for small alkyl iodides, reflecting the non-statistical behavior of dissociation on the repulsive potential energy surface. In the photodissociation of CH_2I_2, however, only about 20% of the available energy is released in translational mode, E_t, (see Table 2) at the wavelength studied (304 nm), which shows the similar results to that observed for CH_2BrI molecule.[41] Thus we see that the presence of two C-I chromophores produces a quite inefficient energy disposal to the translational motion of photofragments. Two limiting impulsive models of photodissociation proposed by Busch and Wilson[42] allow the crude estimation of energy partitioning between internal and translational modes. The rigid radical limit assumes the CH_2I radical as a rigid body so that only rotational excitation can occur during fragmentation. In this limit no vibrations of the radical are excited, and the maximum possible recoil energy is achieved. Assuming that the excited state CH_2I_2 geometry is little changed from the ground state, the rigid radical model predicts a rotational excitation of 0.77 of the available energy. In the soft radical limit, the carbon atom is assumed to be so weakly attached to the rest of the alkyl fragment in relation to the sharp C-I repulsion that it alone initially absorbs the energy as the fragments repel one another. The carbon atom then recoils into the rest of the radical, ex-

Table 3. Relative quantum yield, anisotropy parameter, and assignment for the dissociation channels observed for the photodissociation of CH_2I_2

Iodine state	λ_{ex} nm	Quantum Yield, Φ	Anisotropy parameter, β	Transition type
I	304.67	0.75	0.4	$\parallel (B_1\sigma \leftarrow {}^1A_1)$
				$\parallel (B_1\Pi \leftarrow {}^1A_1)$

accessible states of I_2. For CH_2I_2 the I_2 molecular channel is,

citing the vibrational and rotational degrees of freedom of the radical fragment. The partitioning of energy between translational and internal excitation is determined by simple conservation of energy and momentum. In this way the soft radical limit gives the minimum possible recoil energy for a given available energy.

The $<E_{int}>/E_{avl}$ values calculated from each model are summarized in Table 2. The experimental results show that the fraction of the available energy which goes into internal excitation of the alkyl fragment is about 80% for the photodissociation of CH_2I_2. This indicates that the dissociation dynamics of CH_2I_2 in both I and I* channels is an intermediate of soft and rigid radical limits. Of course in CH_2I_2, the coupling between the two iodine atoms requires a change in the soft model. It might be that this coupling is what changes the observed result from those calculated based on the two impulsive models.

There is still a great deal of experimental and theoretical work needed to describe fully the excited state dynamics, lifetime, absorption features, and photodissociation dynamics of CH_2I_2. The present angular distribution and quantum yield studies provide evidence for a high degree of complexity underlying the dissociation dynamics and also indicate that curve-crossing mechanisms play a significant role in the product-state distributions.

Acknowledgment. The financial support of the National Science Foundation is greatly appreciated. K.-W. J greatefully acknowledge the Korea Science and Engineering Foundation for partial support by the Korea-Germany joint research project 1996-1999 and the Korea Research Foundation for support of this research by the non-directed research fund, 1997.

References

1. Riley, S. J.; Wilson, K. R. *Faraday Discuss. Chem. Soc.* **1972**, *53*, 132.
2. Kawasaki, M.; Lee, S. J.; Bersohn, R. *J. Chem. Phys.* **1975**, *63*, 809.
3. van Veen, G. N. A.; Baller, T.; de Vries, A. E.; van Veen, N. *J. A. Chem. Phys.* **1984**, *87*, 405.
4. van Veen, G. N. A.; Baller, T.; de Vries, A. E.; Shapiro, M. *Chem. Phys.* **1985**, *93*, 277.
5. Kang, W. K.; Jung, K. W.; Jung, K.-H.; Hwang, H. J. *J. Phys. Chem.* **1994**, *98*, 1525.
6. Kang, W. K.; Jung, K. W.; Kim, D. C.; Jung, K.-H.; Im, H.-S. *Chem. Phys.* **1995**, *196*, 363.
7. Dzvonik, M.; Yang, S.; Bersohn, R. *J. Chem. Phys.* **1974**, *61*, 4408.
8. Knee, J. L.; Khundkar, L. R.; Zewail, A. H. *J. Chem. Phys.* **1985**, *83*, 1996.
9. Bosch, R. A.; Salhub, D. R. *Mol. Phys.* **1972**, *24*, 289.
10. Fotakis, C.; Martin, M.; Donovan, R. J. *J. Chem. Soc., Faraday Trans. II* **1982**, *78*, 1363.
11. Gedanken, A.; Rowe, M. D. *Chem. Phys.* **1979**, *36*, 181.
12. Hunter, T. F.; Kristjansson, K. S. *Chem. Phys. Lett.* **1982**, *90*, 35.
13. Ito, M.; Huang, P. C.; Kosower, E. M. *Trans. Faraday Soc.* **1961**, *57*, 1662.
14. Koffend, J. B.; Leone, S. R. *Chem. Phys. Lett.* **1981**, *81*, 136.
15. Kroger, P. M.; Demou, P. C.; Riley, S. J. *J. Chem. Phys.* **1976**, *65*, 1823.
16. Okabe, H.; Kawasaki, M.; Tanaka, Y. *J. Chem. Phys.* **1980**, *73*, 6162.
17. Cain, S. R.; Hofmann, R.; Grant, R. *J. Phys. Chem.* **1981**, *85*, 4046.
18. Schmitt, G.; Comes, F. J. *J. Photochem.* **1980**, *14*, 107.
19. Baughcum, S. L.; Leone, S. R. *J. Chem. Phys.* **1980**, *72*, 6531.
20. Baughcum, S. L.; Hofmann, H.; Leone, S. R.; Nesbitt, D. J. *Faraday Discuss. Chem. Soc.* **1979**, *67*, 306.
21. Hwang, H. J.; El-Sayed, M. A. *Chem. Phys. Lett.* **1990**, *170*, 161.
22. Hwang, H. J.; El-Sayed, M. A. *J. Chem. Phys.* **1991**, *94*, 4877.
23. Hwang, H. J.; El-Sayed, M. A. *J. Phys. Chem.* **1992**, *96*, 8728.
24. Hwang, H. J.; El-Sayed, M. A. *J. Chem. Phys.* **1992**, *96*, 856.
25. Freitas, J. E.; Hwang, H. J.; El-Sayed, M. A. *J. Phys. Chem.* **1993**, *97*, 12481.
26. Freitas, J. E.; Hwang, H. J.; El-Sayed, M. A. *J. Phys. Chem.* **1994**, *98*, 3322.
27. Freitas, J. E.; Hwang, H. J.; El-Sayed, M. A. *J. Phys. Chem.* **1995**, *99*, 7395.
28. Griffiths, J. A.; Jung, K.-W.; El-Sayed, M. A. *J. Phys. Chem.* **1996**, *100*, 7989.
29. Jung, K.-W.; Griffiths, J. A.; El-Sayed, M. A. *J. Chem. Phys.* **1995**, *103*, 6999.
30. Cheng, P. Y.; Zhong, D.; Zewail, A. H. *J. Phys. Chem.* **1995**, *99*, 15733.
31. Hwang, H. J.; Griffiths, J. A.; El-Sayed, M. A. *Int. J. Mass Spectrom. Ion Processes* **1994**, *131*, 265.
32. Barry, M. S. D.; Gorry, P. A. *Mol. Phys.* **1984**, *52*, 461.
33. van Veen, G. N. A.; Baller, T.; de Vries, A. E. *Chem. Phys.* **1985**, *97*, 179.
34. Black, J. F.; Powis, I. *Chem. Phys.* **1988**, *125*, 375.
35. Hwang, H. J. Ph. D. Thesis, University of California, Los Angeles, 1991.
36. Godwin, F. G.; Paterson, C.; Gorry, P. A. *Mol. Phys.* **1987**, *61*, 827.
37. Hwang, H. J.; El-Sayed, M. A. *J. Phys. Chem.* **1991**, *95*, 8044.
38. Zhong, J.; Imre, D. G. *J. Chem. Phys.* **1988**, *89*, 309.
39. Kwok, W. M.; Phillips, D. L. *Chem. Phys. Lett.* **1995**, *235*, 260.
40. Pence, W. H.; Baughcum, S. L.; Leone, S. R. *J. Phys. Chem.* **1981**, *85*, 3844.
41. Butler, L. J.; Hintsa, E. J.; Shane, S. F.; Lee, Y. T. *J. Chem. Phys.* **1987**, *86*, 2051.
42. Busch, G. E.; Wilson, K. R. *J. Chem. Phys.* **1972**, *56*, 3626.